Supplementary Materials for 'Halogen fractionation during vapor-brine phase separation revealed by in situ Cl, Br, and I analysis of scapolite from the Yixingzhai gold deposit, North China Craton'

Wen-Sheng Gao[1,2], Xiao-Dong Deng[1*], Lei Chen[3], Li-Zhong Zhang[1,2,4], Yu-Xiang Li[1], Tao Luo[1], Jian-Wei Li[1,2]

[1] State Key Laboratory of Geological Processes and Mineral Resources, China University of Geosciences, Wuhan 430074, China.

[2] School of Earth Resources, China University of Geosciences, Wuhan 430074, China.

[3] MNR Key Laboratory for Exploration Theory & Technology of Critical Mineral Resources, China University of Geosciences Beijing, Beijing, 100083, China

[4] Zijin Mining Group Co Mineral Exploration Institute, Xiamen 361006, China.

Contents

1.1 Sample description

1.2 EPMA analyses of actinolite in the Tietangdong breccia pipe

1.3 The reference materials and reliability of halogen LA-ICP MS analysis

    1.3.1 Reference materials and corresponding analytical method in this study

    1.3.2 The reliability of Cl, Br, and I analysis by LA-ICP MS

1.4 Numerical simulation

    1.4.1 Rayleigh fractionation

    1.4.2 Vapor loss estimation during fluids phase separation

*Corresponding author

Email: dengxiaodong@cug.edu.cn

1.1 Sample description

Table S1 Sample description of scapolite from the Tietangdong breccia pipe

No.	Elevation (m)	Comment	Sample no.	Mineral associations	Analytical methods
1	1300	Scp I	TTD18	Scp + Grt + Di + (Mag)	SEM-EDS/CL/EPMA
2	1300	Scp I	18Scp-3	Scp + Grt + Di + (Mag)	SEM-EDS/CL/EPMA/LA-ICP MS
3	1300	Scp I	18Scp-1	Scp + Grt + Di + (Mag)	SEM-EDS/CL/EPMA/LA-ICP MS/LA-MC-ICP MS
4	830	Scp II	830Scp-5	Scp + Act + Ep + Cal + (Py + Ccp)	SEM-EDS/EPMA/LA-ICP MS
5	830	Scp I	830Scp-13	Scp + Grt + (Mag)	SEM-EDS/EPMA/LA-ICP MS/LA-MC-ICP MS
6	830	Scp II	830Scp-15	Scp + Act + Ep + Cal + (Py + Ccp)	SEM-EDS/EPMA/LA-ICP MS/LA-MC-ICP MS
7	830	Scp II	830Scp-18	Scp + Act + Ep + Cal + (Py + Ccp)	SEM-EDS/EPMA/LA-ICP MS
8	510	Scp I/Scp II	T510-6	Scp + Act + Ep + Cal + (Py + Ccp)	SEM-EDS/CL/EPMA/LA-ICP MS/LA-MC-ICP MS
9	358	Scp II	T601-152	Scp + Act + Ep + (Py + Ccp)	SEM-EDS/EPMA/LA-ICP MS
10	328.7	Scp I	T601-181.3	Scp (plagioclase replaced) + (Mag)	SEM-EDS/EPMA/LA-ICP MS/LA-MC-ICP MS

Abbreviation: *Scp*-scapolite, *Grt*-garnet, *Di*-diopside, *Act*-actinolite, *Ep*-epidote, *Cal*-calcite, *Mag*-magnetite, *Py*-pyrite, *Ccp*-chalcopyrite.

1.2 EPMA analyses of actinolite in the Tietangdong breccia pipe

Electron probe microanalysis of actinolite was conducted using a JEOL JXA-8230 Superprobe at the GPMR. The analysis was performed using a 15 kV accelerating voltage and 20 nA beam current with 3–5 μm diameter. Counting times on the peak positions were 10 seconds for all elements, except for F and Cl, which used 30 seconds. The background was measured on both sides of the peak for half of the peak time. The Kα line was chosen for Na, Al, Si, Mg, Fe, Mn, K, Ca, Ti, Cl, and F. Detection limits of all the elements were approximately 50–200 ppm, except for Cl (30–40 ppm) and Al (1100 ppm). Natural mineral standards include albite (Na, Si, and Al), K-feldspar (K), plagioclase (Ca), tugtupite (Cl), pyrope (Mg), rutile (Ti), hematite (Fe), rhodonite (Mn), and fluorite (F). The USNM R6600-1 scapolite (Cl: 1.43 wt%; Jarosewich et al. 1980) was used as a secondary standard. The raw data were corrected using the internal ZAF routine. Measured values of USNM R6600-1 are 1.43 ± 0.03 wt% for Cl (n=5, 2σ).

The results are listed in Table S3. The analyzed amphiboles are classified into actinolite (n=17/19; Fig. S1a and Table S3) and have Cl contents of 0.008–0.122 wt%. Furthermore, the Cl contents of all actinolite increase with increasing FeO (Fig. S1b).
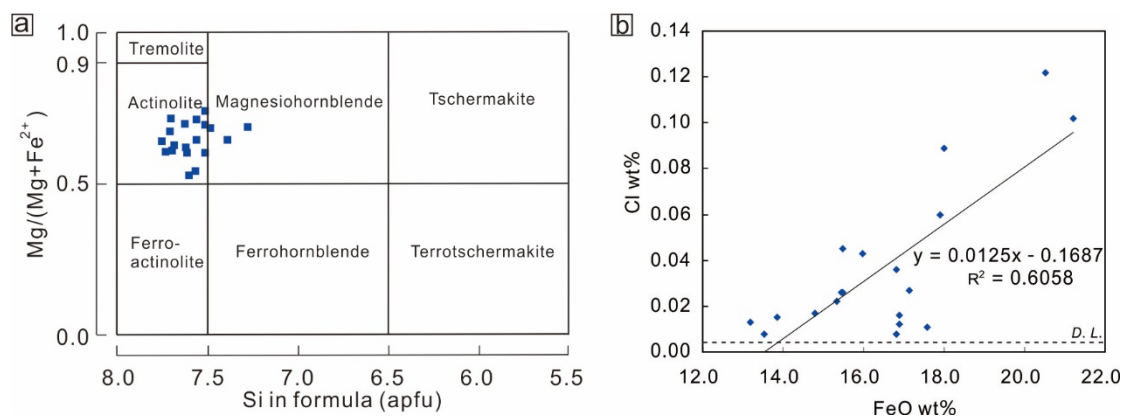
Fig. S1 (a) Classification of amphiboles from the Tietangdong breccia pipe (after Leake et al. 1997). (b) FeO vs. Cl contents of amphiboles. Note that the detection limit of Cl is ca. 40 ppm. *Apfu*- atom per formula unit. D. L.- detection limit.

Table S2 in separate Excel file.

Table S3 EPMA results (wt%) of amphiboles from the Tietangdong breccia pipe

Sample n.o.	15B-1	15B-2	15B-3	15B-4	15B-5	15B-6	15B-7	15B-8	15B-9	15B-10	15B-11	15B-13	15B-14	15B-15	441B-16	441B-17	441B-18	441B-19	441B-20
SiO_2	52.13	50.20	51.81	52.10	52.09	52.25	51.20	52.95	51.21	50.86	49.45	52.95	52.02	52.28	52.93	51.44	51.47	51.40	50.98
Al_2O_3	1.70	3.55	2.49	1.92	1.72	1.91	2.52	1.42	1.89	2.22	4.35	1.86	2.87	2.84	1.41	1.82	2.24	3.03	2.77
TiO_2	0.08	0.05	0.12	0.11	0.11	0.08	0.07	0.09	0.03	0.06	0.07	0.07	0.13	0.14	0.02	[a]b.d.l.	0.02	0.06	0.01
FeO	16.82	17.58	17.14	16.88	16.88	14.78	15.47	15.35	21.20	20.53	15.97	13.18	13.53	13.86	15.44	17.91	16.82	15.47	18.00
MgO	12.87	12.72	13.04	12.82	13.13	14.75	14.28	14.64	10.85	11.09	13.54	15.47	15.44	15.12	13.55	12.03	13.00	13.83	11.96
MnO	0.82	0.83	0.54	0.96	0.54	0.63	0.47	0.41	0.76	0.61	0.47	0.49	0.65	0.66	1.57	1.95	1.51	1.22	1.70
CaO	11.87	12.05	12.06	11.96	12.16	12.28	12.34	12.26	12.02	12.00	12.25	12.34	12.37	12.15	12.29	12.20	12.25	12.31	12.15
Na_2O	0.32	0.28	0.28	0.30	0.28	0.22	0.28	0.23	0.18	0.30	0.48	0.25	0.29	0.33	0.13	0.16	0.20	0.27	0.21
K_2O	0.06	0.06	0.08	0.06	0.07	0.10	0.10	0.12	0.17	0.21	0.20	0.11	0.10	0.15	0.08	0.15	0.13	0.13	0.20
Cl	0.01	0.01	0.03	0.01	0.02	0.02	0.03	0.02	0.10	0.12	0.04	0.01	0.01	0.02	0.03	0.06	0.04	0.05	0.09
F	b.d.l.	b.d.l.	b.d.l.	0.17	0.20	0.11	0.01	0.16	b.d.l.	b.d.l.	0.04	0.07	b.d.l.	0.10	b.d.l.	0.05	b.d.l.	b.d.l.	0.02
Total	96.68	97.33	97.58	97.20	97.09	97.08	96.75	97.58	98.40	97.96	96.83	96.77	97.38	97.60	97.42	97.72	97.66	97.76	98.05
apfu[b]																			
Si	7.73	7.39	7.6	7.69	7.68	7.62	7.51	7.71	7.60	7.56	7.28	7.70	7.51	7.56	7.76	7.61	7.56	7.48	7.51
Al	0.30	0.62	0.43	0.33	0.30	0.33	0.44	0.24	0.33	0.39	0.75	0.32	0.49	0.49	0.24	0.32	0.39	0.52	0.48
Ti	0.01	0.01	0.01	0.01	0.01	0.01	0.01	0.01	0.00	0.01	0.01	0.01	0.01	0.02	0.00	0.00	0.00	0.01	0.00
Fe	2.09	2.16	2.10	2.08	2.08	1.80	1.90	1.86	2.63	2.55	1.97	1.60	1.63	1.68	1.89	2.22	2.07	1.88	2.22
Mg	2.84	2.79	2.85	2.82	2.89	3.21	3.12	3.18	2.4	2.46	2.97	3.35	3.32	3.26	2.96	2.65	2.85	3.00	2.63
Mn	0.10	0.10	0.07	0.12	0.07	0.08	0.06	0.05	0.10	0.08	0.06	0.06	0.08	0.08	0.19	0.24	0.19	0.15	0.21
Ca	1.89	1.90	1.90	1.89	1.92	1.92	1.94	1.91	1.91	1.91	1.93	1.92	1.91	1.88	1.93	1.93	1.93	1.92	1.92
Na	0.09	0.08	0.08	0.09	0.08	0.06	0.08	0.06	0.05	0.09	0.14	0.07	0.08	0.09	0.04	0.05	0.06	0.07	0.06
K	0.01	0.01	0.02	0.01	0.01	0.02	0.02	0.02	0.03	0.04	0.04	0.02	0.02	0.03	0.01	0.03	0.03	0.03	0.04

Cl	0.00	0.00	0.01	0.00	0.00	0.00	0.01	0.01	0.03	0.03	0.01	0.00	0.00	0.00	0.01	0.02	0.01	0.01	0.02
F	0.00	0.00	0.00	0.08	0.09	0.05	0.00	0.07	0.00	0.00	0.02	0.03	0.00	0.05	0.00	0.02	0.00	0.00	0.01
OH	2.00	2.00	1.99	1.92	1.90	1.94	1.99	1.92	1.97	1.97	1.97	1.97	2.00	1.95	1.99	1.96	1.99	1.99	1.97
Fe^{2+}	1.87	1.57	1.78	1.84	1.75	1.41	1.40	1.56	2.20	2.12	1.39	1.36	1.19	1.34	1.67	1.79	1.60	1.40	1.76
$Mg/(Mg+Fe^{2+})$	0.60	0.64	0.62	0.61	0.62	0.69	0.69	0.67	0.52	0.54	0.68	0.71	0.74	0.71	0.64	0.60	0.64	0.68	0.60
Mineral	actinolite	Magnesio-hornblende	actinolite	actinolite	actinolite	actinolite	actinolite	actinolite	actinolite	actinolite	magnesio-hornblende	actinolite	actinolite	actinolite	actinolite	actinolite	actinolite	actinolite	actinolite

[a]b.d.l. = below the detection limit.

[b]apfu = atom per formula unit.

The software package developed by Locock (2014) is used to calculate the formula of amphiboles. It follows the set of recommendations approved by the Commission on New Minerals Nomenclature and Classification (CNMNC) of the International Mineralogical Association (IMA), which was published by Hawthorne et al. (2012).

1.3 The reference materials and reliability of halogen LA-ICP MS analysis

1.3.1 Reference materials and analytical method in this study

In this study, scapolite ON70 from Mpwapwa, Tanzania, was selected as a primary standard. Recommended reference values for Cl (1.94 wt% Cl) and Br (1877 ppm) for the ON70 scapolite standard have been established using μ-SXRF and EPMA method (Evans et al. 1969; Teertstra and Sherriff 1997; Zhang et al. 2017).

Scapolites AF5 and AF8 from Afghanistan were analyzed by NH_4HF_2 digestion and ICPMS analysis for Cl, Br, and I at the State Key Laboratory of Geological Processes and Mineral Resources, China University of Geosciences, Wuhan. For the ICPMS analyses, 100 mg of scapolite powder was mixed with 400 mg of NH_4HF_2 in a 15 ml screw-top Teflon vessel and then placed in an oven at 220°C for 2 h. Upon cooling, the digested cake was transferred to a polyethylene bottle and then diluted to 25 g via 5% v/v NH_4OH solution. 10 µl of an internal standard solution of Te (10 µg/ml) was added to 1 ml of the supernatant solution of the digested sample in a new polyethylene tube. The supernatant was then analyzed using an Element XR inductively coupled plasma sector field mass spectrometer. More details of the method can be found in He et al. (2019). Detection limits for this method are 5 ppm for Cl, 15 ppb for Br, and 5 ppb for I (He et al. 2019). The analytical results of AF5 and AF8 are 7.12 wt% Cl, 661 ppm Br, 106 ppm I, and 7.16 wt% Cl, 148 ppm Br, 28.4 ppm I, respectively.

1.3.2 The reliability of Cl, Br, and I analysis by LA-ICP MS

The analytical parameters of the LA-ICP MS are listed in Table S5. The results

of Cl, Br, and I analysis by LA-ICP MS are reliable based on the following:

(1) LA-ICPMS single-spot analysis of scapolite grains yielded flat and smooth

spectra, indicating the homogeneous distribution of halogens in scapolite and

the absence of halogen-bearing micro-inclusions (Fig. S2a).

(2) Hammerli et al. (2013) reported an observation of significant spurious

interference ^{79}Br isotope as compared to ^{81}Br. Nevertheless, the Br contents

corrected by the intensity of ^{79}Br and ^{81}Br are approximately identical within

their 2σ uncertainty (Fig. S2b), demonstrating that negligible polyatomic

species interfere with the ^{79}Br and ^{81}Br signals by our analytical method.

(3) The chlorine contents on the same spot of scapolite detected by EPMA and LA-

ICP MS overlap within their 2σ uncertainty (Fig. S2c).

(4) The halogen concentrations of the secondary standard (AF5) detected by the

LA-ICP MS overlap with the results measured by the bulk analysis within their

2σ uncertainty (Fig. S2e-f).
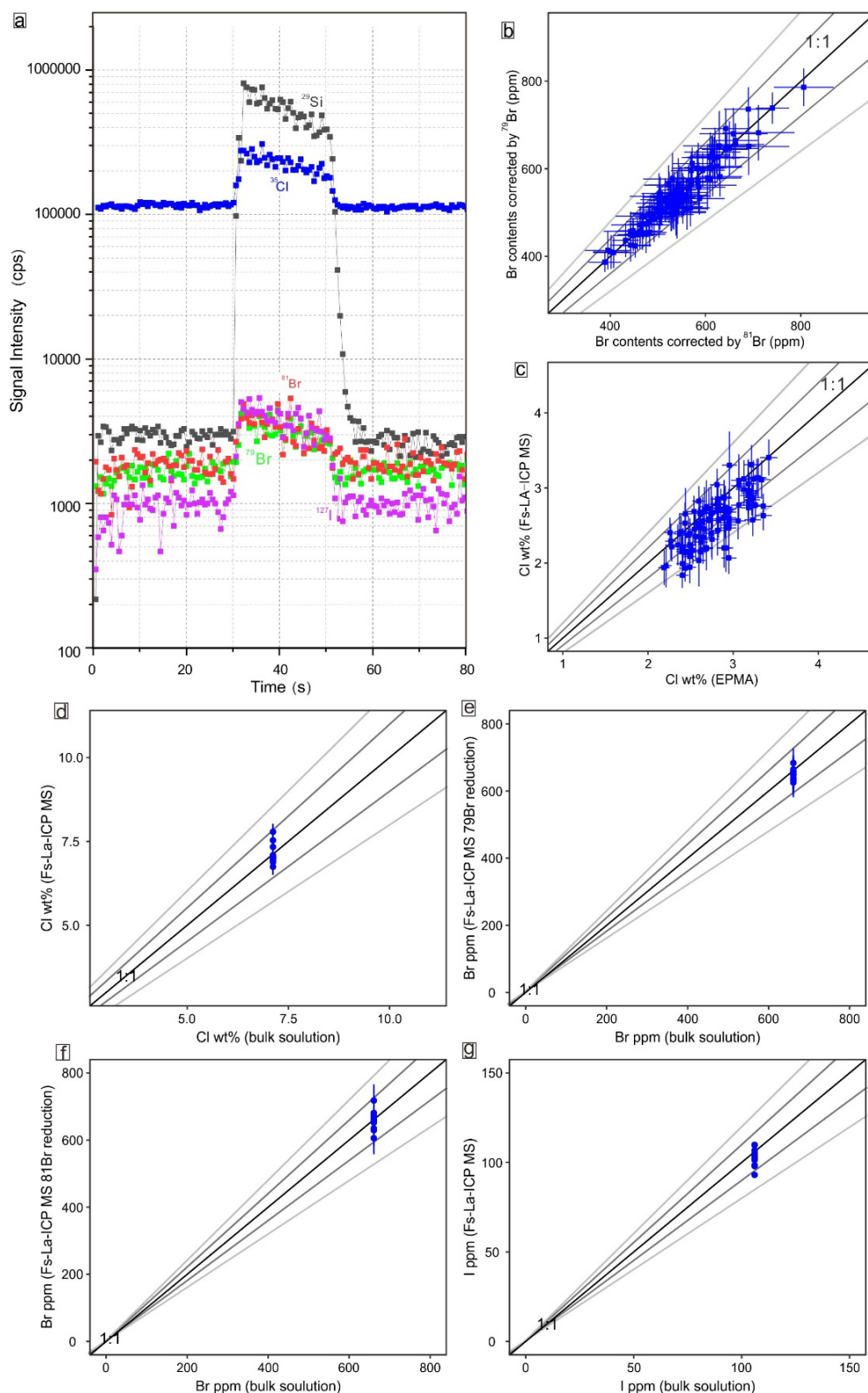

 Table S4 in separate Excel file.

Fig. S2 (a) Representative single spot LA-ICP MS spectra of signals of ^{29}Si, ^{35}Cl, ^{79}Br, ^{81}Br, and ^{127}I. (b) Comparison between Br contents corrected by the intensity of ^{79}Br and ^{81}Br. (c) Chlorine concentrations of scapolite detected by EPMA vs. LA-ICP MS. (e-f) Comparison between halogen concentrations of secondary standard AF5 measured by bulk analysis vs. LA-ICP MS. Note that the error bars indicate 2σ uncertainties. The 10% (dark gray lines) and 20% (gray lines) uncertainty envelopes are also shown.

Table S5 The analytical parameters of LA-ICP MS

Laboratory & sample preparation	
Laboratory name	Institute of Mineral Resource, Chinese Academy of Geological Sciences, Beijing
Sample type/mineral	Scapolite
Sample preparation	Conventional mineral separation, 25 mm-diameter epoxy mounts
Femtosecond laser ablation system	
Make, model & type	J200, Applied Spectra.
Laser wavelength	213 nm
Laser energy set point	5 mJ
Repetition rate	8 Hz
Crater size	50 μm
Carrier gas flow (He)	0.70 l/min
Background	30 s
Ablation	20 s
Washout	70-100 s
ICP-MS Instrument	
Make, model & type	Thermo Element XR Sector-field ICP-MS
Make-up gas flow	1.20 L/min
RF Power	1500 W
ThO^+/Th^+	< 0.3 %
Resolution	medium resolution (m/Δm = 4000)
Isotopes measured	^{29}Si, ^{35}Cl, ^{79}Br, ^{81}Br, and ^{127}I.
Integration type	Average
a ThO/Th and U/Th measured during tuning on a NIST610	
Data processing	
Calibration strategy	Silicon concentrations quantified by EPMA were used as the internal standard for data reduction. The scapolite ON70 and AF8 were used as the external standard for Cl, Br, and I data reduction. Scapolite AF5 used as a secondary standard for quality control.
Reference material information	ON70 (1.94 wt% Cl, 1877 ppm Br; Evans et al. 1969; Teertstra and Sherriff 1997; Zhang et al. 2017); AF8 (with 7.16 wt% Cl, 148 ppm Br, and 28.4 ppm I, determined by bulk analysis, method reported by He et al. 2019); AF5 (7.12 wt% Cl, 661 ppm Br, and 106 ppm I, determined by bulk analysis, method reported by He et al. 2019).
Data processing package used	ICPMSDataCal (Liu et al. 2010).
Quality control/validation	AF5: 7.11 ± 0.59 wt% for Cl, 658 ± 56 ppm for Br, and 102 ± 10 ppm for I (n = 12, 2σ).

1.4 Numerical simulation

1.4.1 Rayleigh fractionation

The Br/Cl and I/Cl values of boiling magmatic-hydrothermal fluid can be quantitatively described as a simple Rayleigh fractionation model (Drummond and Ohmoto 1985):

$$C_{(Br/Cl)}^{Brine} = C_{(Br/Cl)}^{Initial} \times (1 - F_{Vapor})^{\wedge}(1/K_{D(Br/Cl)}^{Brine-Vapor} - 1) \qquad (S1)$$

$$C_{(I/Cl)}^{Brine} = C_{(I/Cl)}^{Initial} \times (1 - F_{Vapor})^{\wedge}(1/K_{D(I/Cl)}^{Brine-Vapor} - 1) \qquad (S2)$$

The initial Br/Cl and I/Cl values of hydrothermal fluid are set at Br/Cl = $1.5/1.8/2.0 \times 10^{-3}$ and I/Cl = $16/30/55 \times 10^{-6}$. These Br/Cl and I/Cl values are typical halogen ratios of magmatic-hydrothermal fluid (Böhlke and Irwin 1992; Irwin and Roedder 1995; Kendrick et al. 2001ab). The Br/Cl and I/Cl exchange coefficients ($K_{D(Br/Cl)}^{Brine-Vapor}$ and $K_{D(I/Cl)}^{Brine-Vapor}$) between brine and vapor are similar because of the similar behavior between Br and I during phase separation of hydrothermal fluid. They are calculated based on the equations from Liebscher et al. (2006) (equations S3 and S4). $D_{Cl}^{Brine-Vapor}$ in equation S3 is the Cl partition coefficients between brine and vapor (equation S5). $D_{Cl}^{Brine-Vapor}$ is related to temperature and pressure and can be calculated based on the vapor-liquid coexistence curve of the H_2O-NaCl system (Driesner and Heinrich 2007). In our simulation, $K_{D(Br/Cl)}^{Brine-Vapor}$ and $K_{D(I/Cl)}^{Brine-Vapor}$ are near 2.3 (Fig. S3a), which are calculated at ~580°C/45MPa (K = 2.26) and ~450°C/30MPa (K = 2.27). These pressure and temperature parameters in our simulation are equal to the conditions of the scapolite formation in the Tietangdong breccia pipe.

$$K_{D(Br/Cl)}^{Brine-Vapor} = 0.349 \times \ln[1.697 \times D_{Cl}^{Brine-Vapor} \text{ -1}) + e^{(1/0.394)}] \qquad (S3)$$

$$K_{D(I/Cl)}^{Brine-Vapor} = 0.349 \times \ln[1.697 \times D_{Cl}^{Brine-Vapor} \text{ -1}) + e^{(1/0.394)}] \qquad (S4)$$

$$D_{Cl}^{Brine-Vapor} = D_{Cl}^{Brine} / D_{Cl}^{Vapor} \qquad (S5)$$

Finally, based on equations S1 and S2, the calculated Br/Cl and I/Cl values of brine gradually increase with the increase of the vapor separation. Those values can be up to 18×10^{-3} of Br/Cl and 500.0×10^{-6} of I/Cl at 98% vapor loss (Fig. S3b). The simulation results are listed in Table S6.

1.4.2 Vapor loss estimation during fluids phase separation

The "vapor loss" is calculated based on mass balance (equation 3) and the X-P-V-T (salinity, pressure, volume, and temperature) diagram of the NaCl-H$_2$O system (Driesner and Heinrich 2007).

$$\text{Mass}_{(initial)} \times \text{salinity}_{(initial)} = \text{Mass}_{(liquid)} \times \text{salinity}_{(liquid)} + \text{Mass}_{(vapor)} \times \text{salinity}_{(vapor)} \qquad (3)$$

We assumed that the initial hydrothermal fluids in the Tietangdong breccia pipe were derived from associated porphyry granite, which had a salinity (salinity$_{(initial)}$) of 5 wt% NaCl eq. If the initial hydrothermal fluid phase separated at 540–590°C and 40–60 MPa (the P-T conditions of Scp I formation), it will evolve to ~ 7–10 wt.% (Mass$_{(liquid)}$) brine with a salinity (salinity$_{(liquid)}$) of 40–60 wt% NaCl eq. and ~ 90–93 wt.% (Mass$_{(vapor)}$) vapor with a salinity (salinity$_{(vapor)}$) of 0.1–1.5 wt% NaCl eq. based on the X-P-V-T (salinity, pressure, volume, and temperature) diagram of the NaCl-H$_2$O system. The simulation results are listed in Table S7.
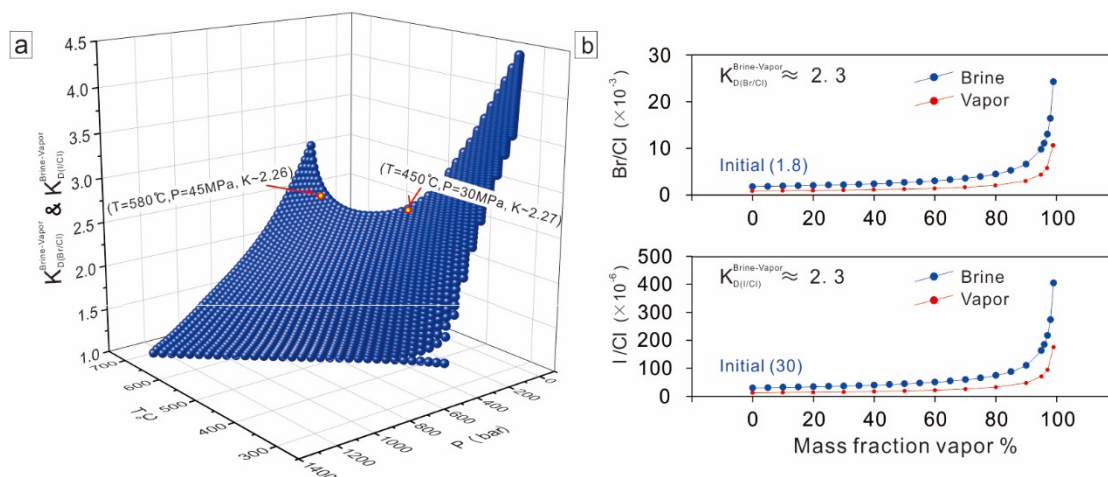
Fig. S3 Rayleigh fractionation model of Br/Cl and I/Cl during hydrothermal fluids phase separation. (a) The exchange coefficients of Br/Cl and I/Cl between brine and vapor depend on the temperature and pressure of hydrothermal fluids (Liebscher et al. 2006). For T = 580°C/P = 45MPa and T = 450°C/P = 30MPa, the corresponding $K_{D(Br/Cl)}^{Brine-Vapor}$ (= $K_{D(I/Cl)}^{Brine-Vapor}$) are 2.26 and 2.27, respectively. (b) Br/Cl and I/Cl values of the brine and vapor phases are associated with the degree of vapor loss during hydrothermal fluids phase separation.

Table S6 Rayleigh fractionation model of molar Br/Cl and I/Cl values in the brine phase during the hydrothermal fluid phase separation

$C_{Br/Cl}^{Initial}$ ($\times10^{-3}$)		$C_{I/Cl}^{Initial}$ ($\times10^{-6}$)		$C_{Br/Cl}^{Initial}$ ($\times10^{-3}$)		$C_{I/Cl}^{Initial}$ ($\times10^{-6}$)		$C_{Br/Cl}^{Initial}$ ($\times10^{-3}$)		$C_{I/Cl}^{Initial}$ ($\times10^{-6}$)	
1.5		16		1.8		30		2.0		55	
$C_{Br/Cl}^{Brine}$ ($\times10^{-3}$) Brine/Vapor	F_{Vapor}	$C_{I/Cl}^{Brine}$ ($\times10^{-6}$) Brine/Vapor	F_{Vapor}	$C_{Br/Cl}^{Brine}$ ($\times10^{-3}$) Brine/Vapor	F_{Vapor}	$C_{I/Cl}^{Brine}$ ($\times10^{-6}$) Brine/Vapor	F_{Vapor}	$C_{Br/Cl}^{Brine}$ ($\times10^{-3}$) Brine/Vapor	F_{Vapor}	$C_{I/Cl}^{Brine}$ ($\times10^{-6}$) Brine/Vapor	F_{Vapor}
20.3/8.9	0.99	216/94	0.99	24.3/10.6	0.99	405/177	0.99	27/11.8	0.99	743/324	0.99
13.7/6.0	0.98	146/64	0.98	16.4/7.2	0.98	274/120	0.98	18.3/8.0	0.98	502/219	0.98
10.9/4.8	0.97	116/51	0.97	13.1/5.7	0.97	218/95	0.97	14.5/6.4	0.97	399/174	0.97
9.3/4.1	0.96	99/44	0.96	11.1/4.9	0.96	185/81	0.96	12.3/5.4	0.96	339/148	0.96
8.2/3.6	0.95	87/38	0.95	9.8/4.3	0.95	163/71	0.95	10.9/4.8	0.95	299/130	0.95
5.5/2.4	0.9	59/26	0.9	6.6/2.9	0.9	110/48	0.9	7.4/3.3	0.9	202/88	0.9
4.4/2.0	0.85	47/21	0.85	5.3/2.4	0.85	88/39	0.85	5.8/2.6	0.85	161/70	0.85
3.7/1.7	0.8	40/18	0.8	4.5/2.0	0.8	75/33	0.8	5/2.2	0.8	137/60	0.8
3.3/1.5	0.75	35/16	0.75	3.9/1.7	0.75	66/29	0.75	4.4/2.0	0.75	120/53	0.75
3/1.4	0.7	32/14	0.7	3.6/1.6	0.7	59/26	0.7	4/1.8	0.7	109/48	0.7
2.7/1.2	0.65	29/13	0.65	3.3/1.5	0.65	54/24	0.65	3.6/1.6	0.65	100/44	0.65
2.5/1.1	0.6	27/12	0.6	3/1.4	0.6	50/22	0.6	3.4/1.5	0.6	92/40	0.6
2.4/1.1	0.55	25/11	0.55	2.8/1.3	0.55	47/21	0.55	3.1/1.4	0.55	86/38	0.55
2.2/1.0	0.5	24/11	0.5	2.7/1.2	0.5	44/20	0.5	3/1.4	0.5	81/36	0.5
2.1/1.0	0.45	22/10	0.45	2.5/1.1	0.45	42/19	0.45	2.8/1.3	0.45	77/34	0.45
2/0.9	0.4	21/10	0.4	2.4/1.1	0.4	40/18	0.4	2.7/1.2	0.4	73/32	0.4
1.9/0.9	0.35	20/9	0.35	2.3/1.0	0.35	38/17	0.35	2.6/1.2	0.35	70/31	0.35
1.8/0.8	0.3	20/9	0.3	2.2/1.0	0.3	37/17	0.3	2.5/1.1	0.3	67/30	0.3
1.8/0.8	0.25	19/9	0.25	2.1/1.0	0.25	35/16	0.25	2.4/1.1	0.25	65/29	0.25
1.7/0.8	0.2	18/8	0.2	2/0.9	0.2	34/15	0.2	2.3/1.0	0.2	62/27	0.2
1.6/0.7	0.15	18/8	0.15	2/0.9	0.15	33/15	0.15	2.2/1.0	0.15	60/27	0.15

1.6/0.7	0.1	17/8	0.1	1.9/0.9	0.1	32/14	0.1	2.1/1.0	0.1	58/26	0.1
1.5/0.7	0.05	16/7	0.05	1.9/0.9	0.05	31/14	0.05	2.1/1.0	0.05	57/25	0.05
1.5/0.7	0	16/7	0	1.8/0.8	0	30/14	0	2/0.9	0	55/24	0

Table S7 The estimation of vapor loss degree during hydrothermal fluid phase separation

Conditions		salinity (wt% NaCl eq.)		Mass ratios		Conditions		salinity (wt% NaCl eq.)		Mass ratios	
T (°C)	P (MPa)	Vapor	Liquid	Vapor	Liquid	T (°C)	P (MPa)	Vapor	Liquid	Vapor	Liquid
540	40	0.1	61.9	92.1	7.9	440	30	0.1	35.8	86.4	13.6
540	50	0.4	50.4	90.9	9.1	440	31	0.2	33.4	85.5	14.5
540	60	1.5	39.1	90.6	9.4	440	32	0.2	31.0	84.5	15.5
550	40	0.1	64.0	92.4	7.6	440	33	0.3	27.6	82.9	17.1
550	50	0.4	53.9	91.3	8.7	450	30	0.1	42.8	88.5	11.5
550	60	1.1	42.6	90.7	9.3	450	31	0.1	40.6	88.0	12.0
560	40	0.1	66.2	92.6	7.4	450	32	0.2	38.3	87.3	12.7
560	50	0.3	56.7	91.7	8.3	450	33	0.2	36.0	86.6	13.4
560	60	0.9	46.0	90.9	9.1	460	30	0.1	47.8	89.7	10.3
570	40	0.1	68.4	92.8	7.2	460	31	0.1	45.7	89.3	10.7
570	50	0.3	58.8	92.0	8.0	460	32	0.1	44.3	89.0	11.0
570	60	0.7	49.6	91.3	8.7	460	33	0.2	42.1	88.5	11.5
580	40	0.1	69.8	93.0	7.0	470	30	0.1	52.5	90.6	9.4
580	50	0.3	60.8	92.2	7.8	470	31	0.1	50.5	90.3	9.7
580	60	0.6	52.4	91.6	8.4	470	32	0.1	49.2	90.0	10.0
590	40	0.1	71.2	93.1	6.9	470	33	0.1	47.1	89.6	10.4
590	50	0.3	63.0	92.5	7.5						
590	60	0.6	54.3	91.8	8.2						

Initial salinity=5.0 wt% NaCl eq.

References

Böhlke, J.K., and Irwin, J.J. (1992) Laser microprobe analyzes of Cl, Br, I, and K in fluid inclusions: Implications for sources of salinity in some ancient hydrothermal fluids. Geochimica et Cosmochimica Acta, 56(1), 203–225.

Driesner, T., and Heinrich, C.A. (2007) The system H_2O-NaCl. Part I: Correlation formulae for phase relations in temperature-pressure-composition space from 0 to 1000 °C, 0 to 5000 bar, and 0 to 1 X_{NaCl}. Geochimica et Cosmochimica Acta, 71(20), 4880–4901.

Drummond, S.E., and Ohmoto, H. (1985) Chemical evolution and mineral deposition in boiling hydrothermal systems. Economic Geology, 80(1), 126–147.

Evans, B.W., Shaw, D.M., and Haughton, D.R. (1969) Scapolite stoichiometry. Contributions to Mineralogy and Petrology, 24, 293–305.

Hammerli, J., Rusk, B., Spandler, C., Emsbo, P., and Oliver, N.H. (2013) In situ quantification of Br and Cl in minerals and fluid inclusions by LA-ICP-MS: A powerful tool to identify fluid sources. Chemical Geology, 337, 75–87.

Hawthorne, F.C., Oberti, R., Harlow, G.E., Maresch, W.V., Martin, R.F., Schumacher, J.C., and Welch, M.D. (2012) Nomenclature of the amphibole supergroup. American Mineralogist, 97(11–12), 2031–2048.

He T., Hu Z.C., Zhang W., Chen H., Liu Y.S., Wang Z.C., and Hu S.H. (2019) Determination of Cl, Br, and I in geological materials by sector field inductively coupled plasma mass spectrometry. Analytical chemistry, 91, 8109–8114.

Irwin, J.J., and Roedder, E. (1995) Diverse origins of fluid in magmatic inclusions at Bingham (Utah, USA), Butte (Montana, USA), St. Austell (Cornwall, UK), and Ascension Island (mid-Atlantic, UK), indicated by laser microprobe analysis of Cl, K, Br, I, Ba+ Te, U, Ar, Kr, and Xe. Geochimica et Cosmochimica Acta, 59(2), 295–312.

Jarosewich, E., Nelen, J. A., and Norberg, J. A. (1980) Reference samples for electron microprobe analysis. Geostandard Newsletter, 4, 43–47.

Kendrick, M.A., Burgess, R., Pattrick, R.A.D. and Turner, G. (2001a) Halogen and Ar-Ar age determinations of inclusions within quartz veins from porphyry copper deposits using complementary noble gas extraction techniques. Chemical Geology, 177(3), 351–370.

Kendrick, M.A., Burgess, R., Pattrick, R.A.D. and Turner, G. (2001b) Fluid inclusion noble gas and halogen evidence on the origin of Cu-Porphyry mineralising fluids. Geochimica et Cosmochimica Acta, 65(16), 2651–2668.

Leake, B.E., Woolley, A.R., Arps, C.E., Birch, W.D., Gilbert, M.C., Grice, J.D., Hawthorne, F.C., Kato, A., Kisch, H.J., Krivovichev, V.G., and others. (1997) Nomenclature of amphiboles; report of the Subcommittee on Amphiboles of the International Mineralogical Association. Mineralogical Magazine, Volume 61, Issue 405, April 1997, pp. 295–310.

Liebscher, A., Lüders, V., Heinrich, W., and Schettler, G. (2006) Br/Cl signature of hydrothermal fluids: liquid-vapour fractionation of bromine revisited. Geofluids, 6(2), 113–121.

 Commission on new minerals and mineral names. Mineralogical Magazine, 61(405), 295–310.

Liu, Y.S., Hu, Z.C., Zong, K.Q., Gao, C.G., Gao, S., Xu, J., and Chen, H.H. (2010) Reappraisement and refinement of zircon U-Pb isotope and trace element analyses by LA-ICP-MS. Chinese Science Bulletin, 55, 1535–1546.

Locock, A., J. (2014) An Excel spreadsheet to classify chemical analyses of amphiboles following the IMA 2012 recommendations. Computational Geosciences, 62, 1–11.

Teertstra, D.K., and Sherriff, B.L. (1997) Substitutional mechanisms, compositional trends and the endmember formulae of scapolite. Chemical Geology, 136, 233–260.

Zhang, C., Lin, J.R., Pan, Y.M., Feng, R.F., Almeev, R.R., and Holtz, F. (2017) Electron probe microanalysis of bromine in minerals and glasses with correction for spectral interference from aluminium, and comparison with microbeam synchrotron X-Ray fluorescence spectrometry. Geostandards and Geoanalytical Research, 41, 449–457.